Unraveling the Structural Landscape of Chitosan-Based Heparan Sulfate Mimics Binding to Growth Factors: Deciphering Structural Determinants for Optimal Activity

Julia Revuelta, Inmaculada Aranaz, Niuris Acosta, Concepción Civera, Agatha Bastida, Nerea Peña, Dianelis T. Monterrey, Ernesto Doncel-Pérez, Leoncio Garrido, Ángeles Heras, Eduardo García-Junceda, Alfonso Fernández-Mayoralas*

ABSTRACT

Chitosan sulfates have demonstrated ability to mimic heparan sulfates (HS) function. In this context, it is crucial to understand how the specific structural properties of HS domains determine their functionalities and biological activities. In this study, several HS-mimicking chitosans have been prepared in order to mimic the structure of HS-domains that have proved to be functionally significant in cell processes. The results presented herein are consistent with the hypothesis that interactions between sulfated chitosan and GFs are controlled by the combined effect of electrostatic interactions and the conformational adaptation of the polymer. Thus, we found that highly charged O-sulfated **S-CS** and **S-DCS** polysaccharides with a low degree of contraction interacted more strongly with GFs than N-sulfated **N-DCS**, with a higher degree of contraction and a low charge. Finally, the evidence gathered suggest that **N-DCS** would be able to bind to an allosteric zone and is likely to enhance GF signaling activity. This is because the bound protein remains able to bind to its cognate receptor, promoting an effect on cell proliferation as has been shown for PC12 cells. However, **S-CS** and **S-DCS** would sequester the protein decreasing the GF signaling activity by depleting the protein or locally blocking its active site.

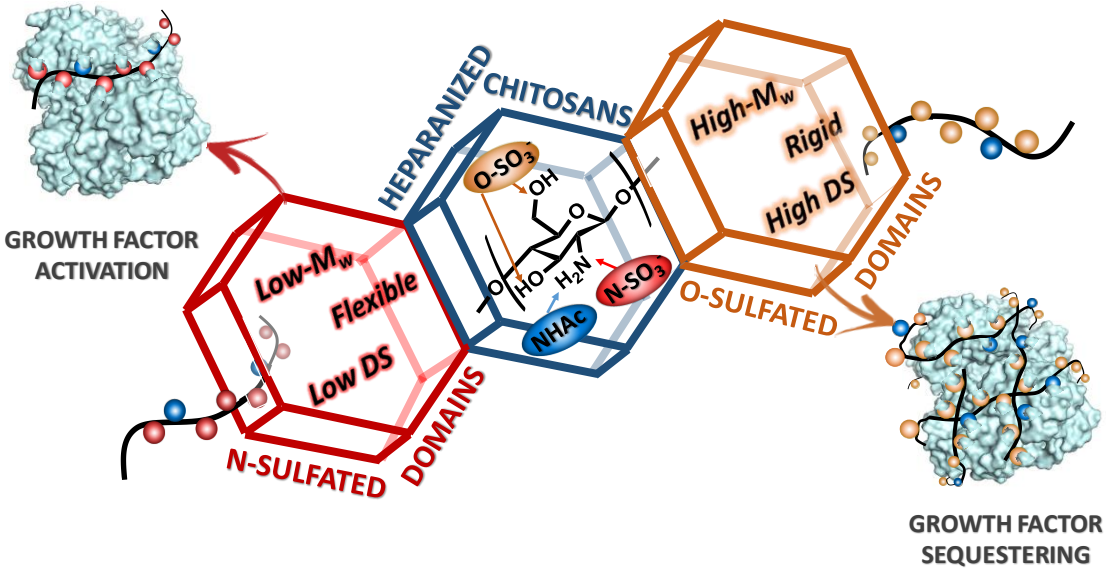

1. INTRODUCTION

Fibroblast growth factors (FGF) play key roles in a variety of relevant biological processes such as cell proliferation, differentiation, cell migration and others.[1] Many of these diverse functions arise from their ability to bind heparan sulfates (HS), important components of heparan sulfate proteoglycans (HSPG) widespread in the extracellular matrix (ECM) and on cell surfaces.[2] After their secretion by cells, GFs bind HS-modified HSPG before reaching their cell-surface receptors. This GF/HS interaction modulates the cellular response, mediating growth factor signaling to cells (Scheme 1A). On the other hand, HSPGs can also shed to provide storage sites in the ECM, protecting growth factors and other proteins such as cytokines, chemokines and morphogens from cleavage by cell-derived metallomatrix and other proteinases (Scheme 1B).[3-4]

***Scheme 1. Schematic illustration of HSPGs roles in GFs regulation. A**. Heparan sulfate proteoglycan (HSPG)-mediated signaling pathways. **B**. Soluble HSPGs as GFs storage sites. The HS chains are symbolized as a string cord with the repeating disaccharide unit (GlcN: black, uronic acid: grey). The circles on the cord represent O-sulfates (orange), N-sulfates (red) and N-acetyl groups (blue).*

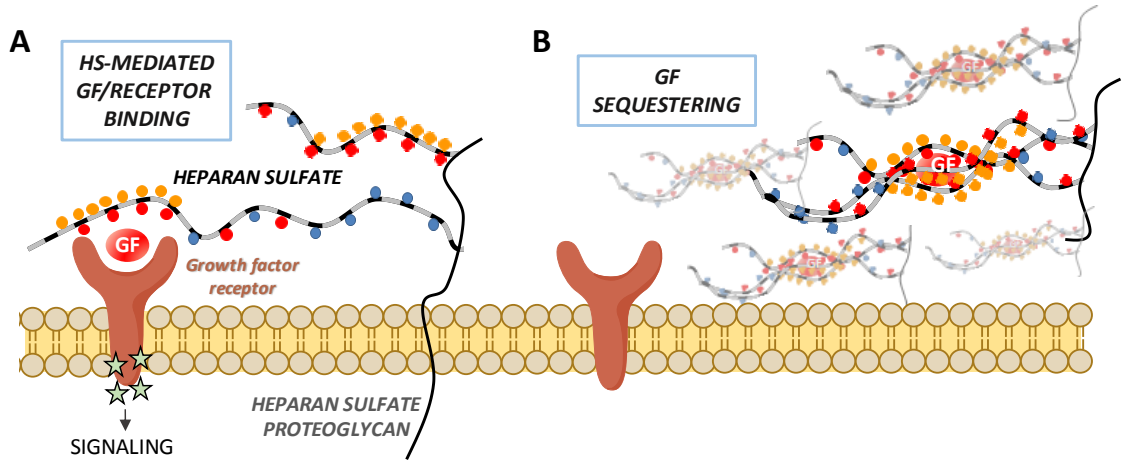

HSs consist of alternating simple subunits of 1→4 linked N-glucosamine (GlcN) and uronic acids (either D-glucuronic, GlcA, or L-iduronic acid, IdoA), which can be sulfated at different positions. Its biosynthesis is a complex multistep process that occurs via polymerization of alternating GlcA and GlcNAc residues and subsequent modification of the repeated disaccharide units.[5] These modifications include the partial N-deacetylation/N-sulfation of the GlcNAc residues followed by C-5 epimerization of GlcA to iduronic acid and *O*-sulfation at various positions. This represents only the first level of molecular diversity in HS chains (Figure 1).[6]

Despite the apparent heterogeneity of these modifications, post-polymerization transformations occur with high specificity, generating *regions* or *domains* throughout the HS polymer which are of defined size, spacing and general composition (Figure 1) known as NS-domains (NS), NA domains (NA) and transition zones (NS/NA). The NS-domains are regions enriched in *N*-sulfate GlcN, whilst NA domains have stretches of unmodified N-acetylated disaccharide units. Both regions are interconnected via interspacing domains composed of alternating *N*-sulfated and *N*-acetylated disaccharides (transition zone).[7] The multiple combinations of these domains generate the second level of diversity of these biopolymers.

Recent studies have demonstrated that the tight and specific binding between HS and growth factors is not solely regulated by sulfation profile and GlcA/IdoA relationship, both the structure of the highly NS-domains and the organization/availability of such domains within the HS chains are determinant on FGF-2 signaling.[8-9]

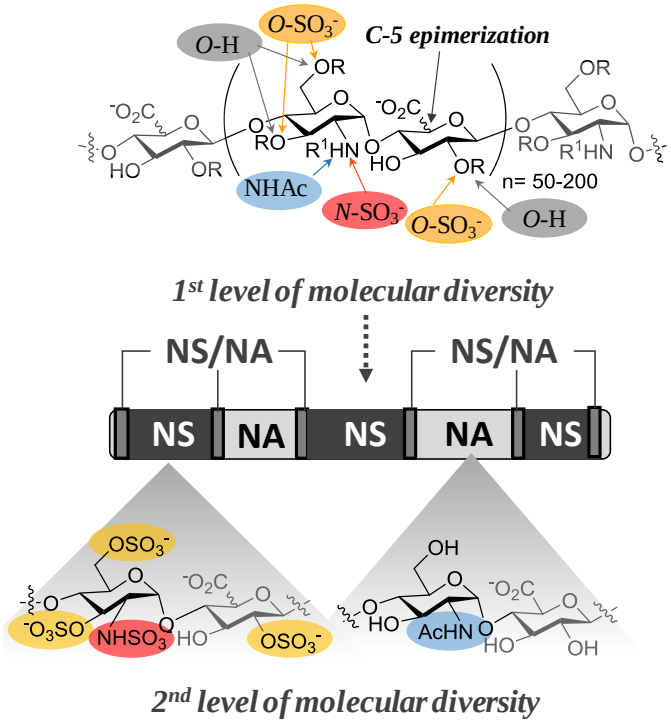

Figure 1. *Dual molecular diversity in HS chains. Micro-heterogeneities resulting from the various uronic acid and sulfation motifs generate a first level of molecular diversity. The distribution of NS-domains, NA-domains and transition zones of variable length leads to a second level of molecular diversity.*

Nevertheless, the plethora of combinations of these domains complicates the detailed understanding of HS sulfation patterning and the direct determination of structure-function relationships of HS motifs. It is important to note that, unlike other instances where biological information is encrypted as linear sequences in molecules such as DNA, HS chains are generated through a non-template driven processes and may also be dynamically remodeled in response to variations in the environment. These modifications provide additional variability with regard to biological functions[10] and are typically characterized by

the degradation of the chains by the heparanase[11] or by modification of the sulfation patterns via *O*-sulfatases.[12]

For these reasons, deciphering the structural code of HSs and their dynamic nature generation processes are currently very important challenges. Recent efforts have relied on the total synthesis[13] or the chemical[14] or enzymatic[15] modification of HSs. These are expensive and time-consuming procedures that are still challenging. Alternatively, there is a growing interest in the preparation of synthetic glycans[16] and glycomimetics[17] as alternatives to the natural polysaccharides.[18]

Among them, chitosan sulfates have demonstrated the ability to mimic HSs for protein binding,[19] exhibiting intrinsic biological properties towards cell differentiation, proliferation and growth[20-21] and a protective effect against proteolytic digestion of GFs,[22] depending on the sulfation states of the chains.

Herein, chitosan has been modified in order to mimic the structure of NS-domains and the transition zones of HS, the regions that have demonstrated functional significance in cell processes in terms growth factor binding (Figure 2A). It is conceivable to think that in heparanized chitosan mimics, as in natural polysaccharides, selective recognition properties may reside at the domain topology. Our strategy addresses the unmet challenges of how the domain structures orchestrate cellular responses when they are introduced in chitosan sulfate mimetics (Figure 2B).

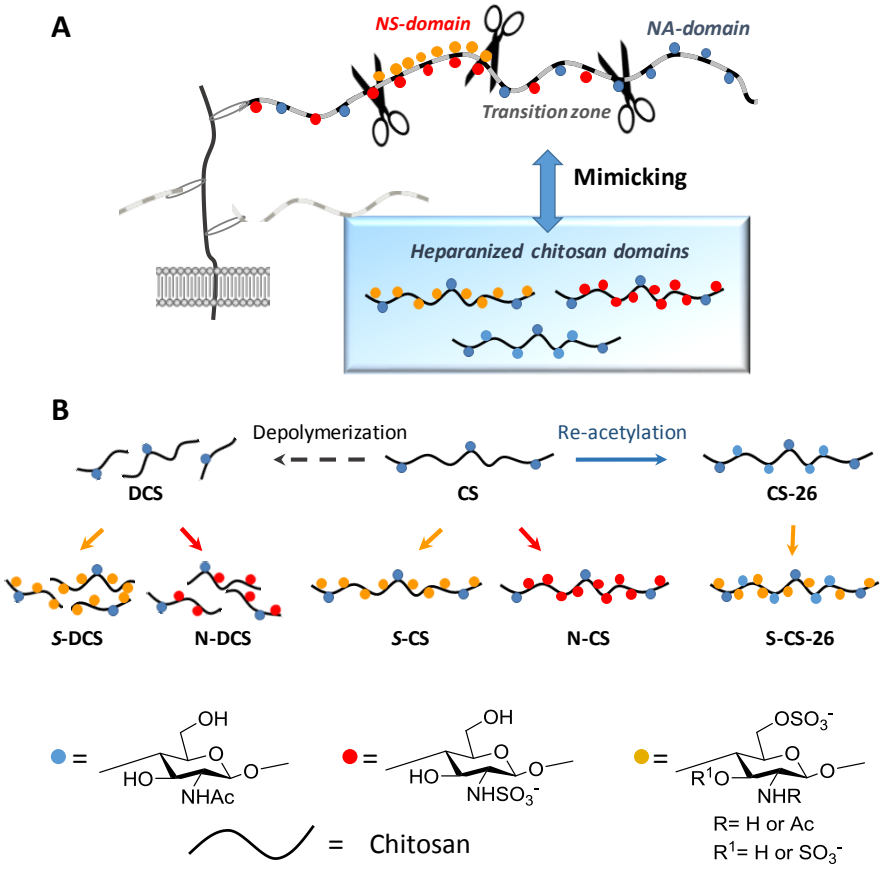

Figure 2. A*. Design of HS-mimicking chitosan.* ***B****. Schematic representation of the CS used in this work. The chitosan chains are symbolized as a string black (***CS***: Chitosan;* ***DCS****: Depolymerized chitosan and* ***CS-26****: Chitosan with an acetylation degree (DA)= 0.26). These have been decorated with NS-domain (O-sulfates or N-sulfates) and NA-domain (N-acetyl) motifs. The circles on the cord represent O-sulfates (orange), N-sulfates (red) and N-acetyl groups (blue). S- and N- indicate the O- or N-sulfation of the polysaccharide.*

2. EXPERIMENTAL SECTION

General methods. Chitosan (**CS**) (see Table S1) was purchased from INFIQUS, S.L. (Spain). **DCS** and **CS-26** were prepared according to previously reported methods (Supporting Information). Heparin was purchased from Alfa-Aesar. FT-IR spectra were recorded with KBr pellets on a Perkin Elmer Spectrum One spectrophotometer. ^{1}H NMR spectra were registered at 400 or 500 MHz and ^{13}C NMR spectra were obtained at 100 or 125 MHz on Varian INOVA and Varian SYSTEM spectrometers, respectively. Elemental analyses were performed in a Heraus CHN-O analyzer. The total degree of acetylation (DA)

was calculated from ^{1}H NMR according to Lavertu et al.[23] The total degree of sulfation (DS) was calculated from elemental analysis of the compounds according to the following equation: Total DS = (S%/32.06)/(N%/14.01). Statistical analysis was performed using Unpaired t-test.

Preparation of *O*-sulfated chitosan. Sulfated chitosans were prepared according to a previously reported method.[20] For example, a solution of **CS** (0.5 g) in formic acid (23 mL) was stirred within 1 h at room temperature. Then DMF (122 mL) was added, followed by another 2 h of stirring. After that, chlorosulfonic acid (1.4 mL) in DMF (8 mL) was dropped slowly into the **CS** solution within 15 min and the mixture was kept at room temperature for 5 h. The resulting yellow solution was poured into a saturated ethanolic solution of anhydrous sodium acetate (300 mL) and the mixture was kept overnight. The obtained precipitate was washed with ethanol/water (4:1) mixture (v/v) and then dissolved in water (45 mL) and the pH value of the solution was adjusted to 7.5. Subsequently, the solution was dialyzed against water and lyophilized to give **S-CS**. This procedure was also applied for the sulfation of **CS-26** and **DCS**, to give **S-CS-26** and **S-DCS** respectively (see Table 1).

Preparation of *N*-sulfated chitosan. N-sulfated chitosans were prepared following the conditions described by Holme et al.[24] For example, **DCS** (1 g) was dispersed in distilled water (30 mL), and treated with Na_2CO_3 (357 mg) and $Me_3N{\cdot}SO_3$ (710 mg). The mixture was heated at 50 °C until a clear viscous solution was formed (~24 h). The cooled mixture was then dialyzed exhaustively against distilled water and then lyophilized to give **N-DCS**. This procedure was also applied for the sulfation of **CS**, to give **N-CS**.

NMR solids. N-15 solid-state NMR measurements were performed on a Bruker Avance™ spectrometer equipped with a wide bore superconductive magnet operating at 9.4 T (N-15 Larmor frequency at 40.56 MHz). Powdered samples were packed in 4 mm ∅

zirconia rotors. The CP/MAS NMR measurements with contact times of 3 ms, repetition rates of 2 s and high-power proton decoupling (75 kHz) were carried out at room temperature, and spinning rates of 5 kHz. Generally, 45,000 scans were averaged unless specified otherwise. The spectra were externally referenced to ammonium chloride (-338.1 ppm) secondary to nitromethane (0.00 ppm).

Molecular weight analysis. The M_w and M_n of the polysaccharides were determined using gel permeation chromatography (GPC). GPC measurements were performed in a Waters 625 LC System pump with a linear ultrahydrogel column (Waters, i.d = 7.8 mm, l = 300 mm) thermostated at 35 °C. Waters 2414 differential refractometer was connected online. 0.04 M sodium dihydrogen phosphate anhydrous-0.06 M disodium hydrogen phosphate anhydrous (pH= 6.8) was used as eluent for chitosan sulfate derivatives. Chitosan samples were eluted using 0.2 M $AcNH_4$-/0.2 M AcOH as eluent. The flow rate was 0.6 mL/min and 20 μL of samples dissolved in the buffer were injected.

Zeta potential. Chitosan sulfates were dissolved (1 mg/mL) in NaCl 1 mM and chitosan were dissolved (1 mg/mL) in AcOH 0.1 M. Zeta potential measurements were performed on a Malvern Zetasizer Nanoseries Nano ZS (Malvern Instruments, Herrenberg, Germany). Each experiment was carried out in triplicate.

DOSY experiments. Diffusion ordered spectroscopy experiments were performed on a 500 MHz VARIAN System, using 16 gradients (2.5–50.0 gauss per cm) with a gradient pulse (d) of 3 ms and a diffusion time (D) of 150 ms.16 gradients between 2.5 and 50.0 gauss per cm with a gradient pulse (δ) of 3 ms, a diffusion time (Δ) 150 ms.

Circular dichroism spectroscopy. Circular dichroism spectra were acquired in a Jasco-710 dichrograph, previously calibrated with D-10-camphorsulphonic acid. Measurements were performed in 1 cm Quartz Hellma cuvettes cells at 25 °C. The temperature was kept

constant with a Neslab bath RTE-111. Five accumulations were acquired for each spectrum. The ellipticity was measured with a 1 nm bandwidth and 2 s response. The CD spectra were recorded between 200 and 240 nm.

Determination of Intrinsic Viscosity and "*Degree of Contraction*". The dynamic viscosity of dilute polysaccharide solutions was measured using an AMVn automated rolling ball micro-viscometer (Anton Paar, Ostfildern, Germany) with a programmable tube angle based on the principle of the rolling ball time. The intrinsic viscosity [η] in water ($[\eta]_{H_2O}$) and 0.1 M NaCl ($[\eta]_{NaCl}$), both at pH 7.0, was determined as previously described. The degree of coil contraction was thus expressed as the following ratio: $[\eta]_{H_2O}/[\eta]_{NaCl}$.

Protein binding assays. Heparin or chitosan derivatives (**S-CS**, **S-DCS**, **N-DCS** and **S-CS-26**, 2 mg/mL) were dissolved in sodium bicarbonate buffer (pH 9.6) and transferred to the wells of Nunc Immobilizer Amino™. Blank wells were incubated with 100 mM ethanolamine in sodium phosphate buffer (pH 9.6) containing hexadecyl-trimethyl ammonium bromide (1 mM). All samples were performed in triplicate. The plate was shaken overnight, then emptied and washed with water. All wells were then blocked by 1 h incubation at 37 °C with 3% BSA in PBS. Then, the cells were washed with PBS-t three times. 100 µL of Growth Factor solution (FGF-2, FGF-1, NT-3, BDNF or EGF from PeproTech, 25 ng/well in PBS) were added to each well. The microplate was incubated with gentle agitation at room temperature for 1 h and washed with PBS containing 1% Tween 20, and water. 100 µL of anti-human (FGF-2, FGF-1, NT-3, BDNF or EGF antibody, 50 ng) was added to the wells. The plate was shaken for 1 h and washed with PBS containing 1% Tween 20, and water. Immediately after the final wash step, dry the slide, and Anti-Rabbit IgG peroxidase is added. The colorimetric assay was used by on Amplex® UltraRed reagent (Ex/Em 568/581 nm).

Isothermal Titration Calorimetry (ITC). These studies were performed at 20 ºC in PBS (100 mM NaCl, 20 mM Na_3PO_4, pH 7.4) by using a Nano ITC calorimeter (TA Instruments). Dilution experiments with **S-CS** and **N-CS** were performed with a starting concentration of polysaccharide in the syringe of 200 μM. For binding studies, a 10 μM solution of FGF-2 (190 μL) was titrated in the reaction cell with a 200 μM solution of **S-DCS** and **N-DCS** respectively. In all cases, buffer composition in the syringe and titration cell was identical. In each experiment, 17 injections of 3 μL were carried out while the protein solution was stirred at a constant speed of 300 rpm. Experiments were performed in duplicates. Experimental curves were analyzed using the software provided by TA instruments.

Preparation of primary neural precursors cells. The neural precursor cells (NPCs) were obtained from striatum E15 rat embryos that were dissected and mechanically dissociated to individual cells. This cell suspension was incubated in NB27 medium containing human FGF-2 (10 ng/mL) and EGF (20 ng/mL; Peprotech, New Jersey, USA)].[25] After about 7 days in this medium floating neurospheres formed were collected by low-speed centrifugation, dissociated by mild trypsinization and passed through a 25-gauge needle, and expanded every 3–4 days.

Neurosphere cell differentiation. After fourth passage, neurospheres were dissociated to individual NPCs and were plating (10^5 cells/well) on 24-well culture plates (Falcon, NJ, USA) pre-treated with poly-l-lysine and laminin (1 mg/mL) to permit cell attachment. Then, NPCs were incubated 10 days for differentiation in NB27 containing growth factors and chitosan sulfates derivatives at tolerated doses. The medium was renewed every third day and finally, the cells were fixed with 2% paraformaldehyde/sucrose in PBS (12 min, 25 °C) for immunocytochemistry.

Preparation of PC-12 cells. The PC-12 rat pheochromocytoma cells [PC¬12 (ATCC® CRL¬1721™)], were used as a cell model for neurotoxicity[26-27] and cell cancer inhibition.[28-29] The PC-12 cells were cultured in DMEM plus 7,5% horse serum and 7.5% bovine serum until treatment. The neurotoxicity in PC12 cells was assayed at densities between $5–10^4$ cells per well and treated by 72 h with the polysaccharides. The MTT assay was used to follow cell growth and viability (Supporting Information).

Cell Growth Inhibition. The PC12 cells were seeded at 10^4 cells/well and allowed to attach for 6 h. After the cells were attached to the substrate, the medium was changed to serum-free DMEM, and the cells were incubated for 48 h. Then the medium was replaced by DMEM plus 1% HS/BS, containing the polysaccharides, in triplicate. The cell growth inhibition of the cells was calculated as follows: % inhibition = 100 - 100[(X - B)/(A - B)] Where A is mean experimental Abs corresponding to cells maintained in DMEM plus serum; B is the mean experimental Abs. from medium free of cells, and X corresponds to experimental Abs. of cells treated with chitosan sulfate variants. Each treatment was assayed in triplicate at least.

Immunocytochemistry. The fixed NPCs were washed with PBS and immunostained as follows: they were incubated for 30 min, at 25°, in PBS containing bovine serum (2%) and 0.1% Triton X100. The cells were then incubated (16 h at 4 °C) in the same mixture containing the primary mouse monoclonal antibody for nestin (Santa Cruz Biotechnology) or rabbit polyclonal antibody for GFAP (Acris) diluted at 1/500. After repeated washing with PBS, the cells were treated with secondary antibody, a goat anti-mouse or anti-rabbit IgG antibody (Molecular Probes) diluted 1/1000 (45 min, 25 °C); Hoechst agent at 10 μg/mL (Sigma) was added for cell nuclei labeling during 10 min at 25 °C, washed three times with PBS, and conserved with glycerol/PBS (1/1). The assays were made three times by

duplicates, in each replicate 40 fields were selected and analyzed by IN Cell Analyzer 1000 Cellular Imaging (General Electric).

3. Results and discussion

3.1. Synthesis and chemical characterization of polysaccharides.

To mimic the structure of the different domains we have prepared polysaccharides with different properties (M_w and DA) and with sulfate residues in the range of natural HSs that bind growth factors.

O-sulfonations of **CS**, **DCS** and **CS-26** were achieved under homogeneous conditions using a chlorosulfonic acid/formic acid system, to produce **S-CS**, ***S*-DCS** and **S-CS-26**.[20] The *N*-sulfated derivatives (**N-CS**, **N-DCS**) were prepared from polysaccharides **CS** and **DCS** using the $SO_3 \cdot NMe_3$ complex as sulfating reagent in the presence of Na_2CO_3.[24] Elemental analysis indicated that chitosans are substituted with sulfate groups in the range of 0.6-1.4 sulfates/monosaccharide (Table 1), which mimic the level of sulfate modification of natural HSs.[30]

Table 1. Sulfation of chitosan.

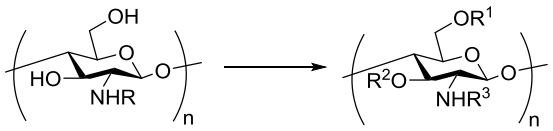

R= H or Ac

S-chitosans: R^1, R^2= SO_3^- or H; R^3= H or Ac
N-chitosans: R^1, R^2= H; R^3= H, Ac or SO_3^-

	Starting chitosan	***Sample***	***Yield***	***DA***[a]	***Total DS_S*** [b]
O-sulfated chitosan	CS	**S-CS**	65%	3.2	1.38
	DCS	**S-DCS**	72%	3.1	1.35
	CS-26	**S-CS-26**	61%	3.5	1.31
N-sulfated	CS	**N-CS**	79%	3.5	0.63

chitosan	DCS	**N-DCS**	81%	3.35	0.65

[a]Degree of acetylation. Calculated according with reference 23; [b]Degree of sulfation. Determined using elemental analysis.

The chemo-selectivity of the sulfonations was analyzed by FTIR spectroscopy (Figure 3A). Spectra of **S-CS** have two peaks that are representative of a *O*-sulfate at approximately 1234 cm^{-1} (ν_{as} O=S=O) and 802.06 cm^{-1} (ν_{as} C-O-S). However, in **N-CS** this last peak is not observed, indicating that the chitosan is sulfated only at the 2-*N* position. This selectivity was corroborated by ^{15}NCP/MAS NMR spectroscopy. In this case, **N-DCS** spectra shows the presence of a signal around -283 ppm corresponding to the sulfamic acid ($NHSO_3$) that is not observed in the **S-DCS** (Figure 3A).

On the other hand, ^{13}C and two-dimensional (2D)-NMR experiments allowed the determination of the regio-selectivity of *O*-sulfonations. For example, HSQC-DEPT spectrum of **S-DCS** (Figure 3B) displayed antiphase signals for both sulfated ($\delta_{H,C}$= 4.25/66.5) and non-sulfated ($\delta_{H,C}$= 3.83/60.0 ppm) CH_2 at position six. Furthermore, two phase signals at $\delta_{H,C}$ = 4.3/78.8 ppm (minor) and at $\delta_{H,C}$ = 3.8/72.8 ppm (major) were attributed to sulfated and non-sulfated CH at position three. In both cases, an estimation of the sulfation degree was carried out by integration of each set of signals with respect to the CH-2 density.[20]

Finally, the net surface electrical charge was estimated by the zeta potential, seeming to be independent of the degree of sulfation (Figure 3C). These results suggest that the structural motifs of the different domains could display a significant effect on the polysaccharide 3D-structure and, therefore, on the surface charge.

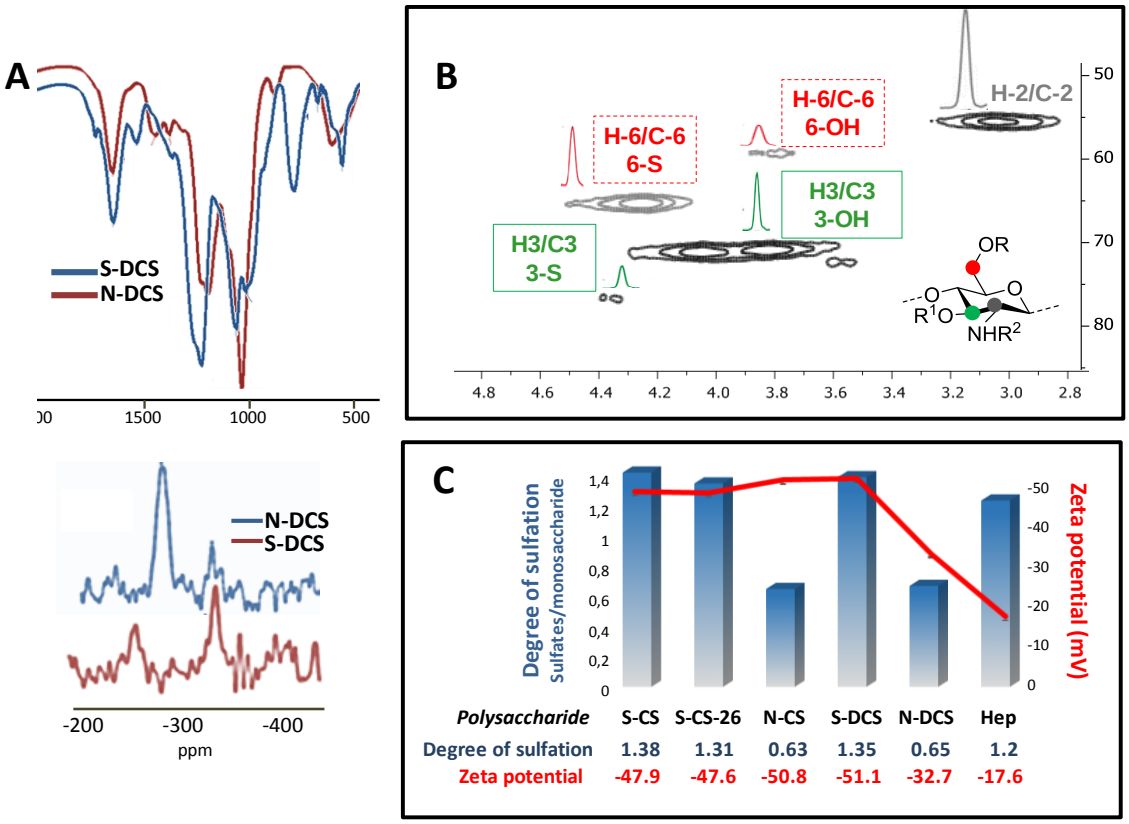

Figure 3. *Characterization of chitosan-based HS-domains mimics.* ***A****. Key regions of IR (top) and 15NCP/MAS NMR (bottom) spectra of* **S-DCS** *(blue) and* **N-DCS** *(brown).* ***B****. Key region of HSQC spectra of polysaccharide* **S-CS**. *Densities enclosed in the color boxes were integrated for sulfation degree estimation: 6-position (dashed red line) and 3-position (solid green line).* ***C****. Degree of sulfation of chitosan sulfates. The red line indicates the zeta-potential values. Their numerical values are indicated at the bottom in red.*

3.2. Conformational analysis of polysaccharides: Physicochemical characterization.

Chitosan sulfates are polyampholytic polymers due to the presence of positive and negative charges randomly distributed along the chain. These charges control the structural and dynamic properties of the polymers and play a crucial role in the binding of polysaccharides with proteins,[31-32] giving rise in several cases, to distinct biological responses.[33] To gain insight into those properties, we have used a panel of biophysical techniques. The intrinsic structures of the polysaccharides were estimated by analysis of two variables, the hydrodynamic volume and the zeta-potential, whilst the "*degree of contraction*" has been employed as an estimation of the intrinsic chain flexibility (Table

2).[34] It is important to note that in polyampholytic polymers, both properties are dependent not only on the net charge but also on the charge distribution through the chain. Moreover, they can exist either as individual chains stabilized by cooperative intra-polymer interaction or as soluble complexes when attractive interactions between different polymer chains take place.[35-36]

Table 2. Chitosan sulfates physicochemical parameters.

Sample	M_w (kDa)[a]	M_n (kDa)[b]	PI[c]	ζ (mV)[d]	η_{H_2O} [e] (mL/g)	η_{NaCl} [e] (mL/g)	η_{H_2O}/η_{NaCl} [f]
***S*-CS**	77.5	34.0	2.28	-47.9	850	88	9.6
S-CS-26	262.3	55.4	4.74	-47.6	1800	130	13.8
***N*-CS**	142.6	36.9	3.85	-50.8	650	68	9.5
***S*-DCS**	52.2	26.2	1.99	-51.1	225	13	17.3
***N*-DCS**	36.0	15.9	2.27	-32.7	450	14	32.0

[a] Mw = weight-averaged molecular mass. [b] Mn= number-averaged molecular mass. [c] PI= Polydispersity index. [d] ζ= Zeta-potential. [e] [η] = intrinsic viscosity (subscript denotes the solvent). Microviscosimetric measurements taken at pH 7.0 in water and 0.1 M NaCl at 37 °C, inclination angle 50°. [f] η_{H_2O}/η_{NaCl} = degree of contraction.

***S*-CS**, ***N*-CS** and ***S*-CS-26** had very different hydrodynamic volumes, according to the M_w determined by gel permeation chromatography (GPC) (Table 2). Dependence on the *N*-substitution degree was evident thus reflecting the existence of important structural changes when the number of free amine groups along the chitosan chain is reduced. Therefore, the relatively low hydrodynamic volume observed for ***S*-CS** in comparison with ***S*-CS-26** and ***N*-CS** could be explained by rigid individual chains stabilized by cooperative intra-polymer electrostatic interactions between the sulfate groups at C-6 and the protonated amino groups on adjacent residues, as previously suggested (Figure 4).[37] The low $[\eta]_{H_2O}/[\eta]_{NaCl}$ ratio in comparison with other charged polysaccharides suggests that this compact conformation of ***S*-CS** may be less sensitive to long-range electrostatic charge screening in the presence of NaCl.[31]

This structure is consistent with the observed behavior when the degree of acetylation reaches 26% (**S-CS-26**). Our results showed that increasing the DA increases the hydrodynamic volume and the $[\eta]_{H_2O}/[\eta]_{NaCl}$ ratio. This can be explained in terms of a more expanded and less rigid conformation due to the decrease in electrostatic interactions between neighboring residues by loss of free amino groups by the acetylation. In turn, the highest hydrodynamic volume implies that **S-CS-26** adopts a less compact structure which suggests the presence of molecular and structural heterogeneity. This is likely due to the block acetyl groups distribution. These results could be supported by the slight decrement on the crystallinity index from 16% of **S-CS** to 11% in the case of **S-CS-26**, estimated from XRD data according to a previously described method.[38]

When chitosan was *N*-sulfated an important increase in hydrodynamic volume was observed, which could be attributed to a chain expansion. However, our results showed that increasing the hydrodynamic volume did not increase the ratio $[\eta]_{H_2O}/[\eta]_{NaCl}$, which suggest that **N-CS** adopts a completely different structure to **S-CS**. Based on these results, we propose that a charge-driven self-association between chains could take place, giving rise to rigid poly-electrolytic complexes (Figure 4).[36,39] In fact, it has been observed that **N-CS** spontaneously forms a hydrogel in aqueous medium at room temperature without any chemical treatment (Figure 4).

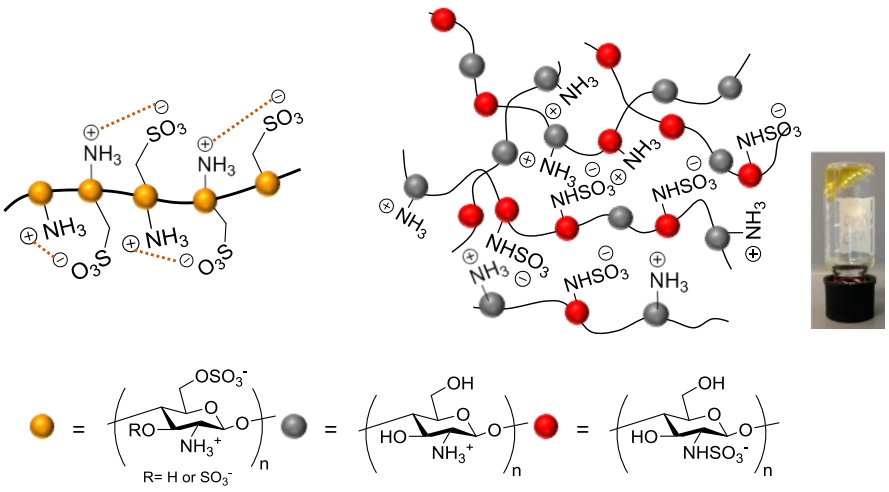

Figure 4. *Schematic illustrations of the proposed structures for* **S-CS** *as individual chains stabilized by cooperative intra-polymer interaction (left) and for* **N-CS** *(right) as soluble complexes when attractive interactions between different polymer chains have taken place (right). An image of the spontaneously formed* **N-CS** *hydrogel is shown.*

Finally, in the case of depolymerized sulfated chitosan (**S-DCS** and **N-DCS**) a different tendency was observed. In this case, the hydrodynamic volume of **N-DCS** is minor than in **S-DCS**, whilst the ratio $[\eta]_{H_2O}/[\eta]_{NaCl}$ increases in *N*-sulfate versus *O*-sulfate. This support previous research suggesting that there is a critical chain length, above which chitosan and its derivatives tend to form stable self-assembled structures.[40]

To gain insight into these proposed structures, isothermal calorimetry (ITC) was used. Dilution enthalpogram for **S-CS** shows the normal effect of a dilution process on non-assembled structures (Figure 5A). In contrast, dilution enthalpogram for **N-CS** is consistent with the presence of self-assembling structures (Figure 5B). Based on results described previously for these systems,[41] the first region of the enthalpogram reflects the result of de-complexation of the cooperative binding, which is ended during the second set of injections. During this set, a dilution process of the polymer chains is also observed. When polymers form stable self-assembled structures, these are resilient to the replacement of polymer chains by hydration molecules, thus resulting in an endothermic dilution process which is observed in the final region.

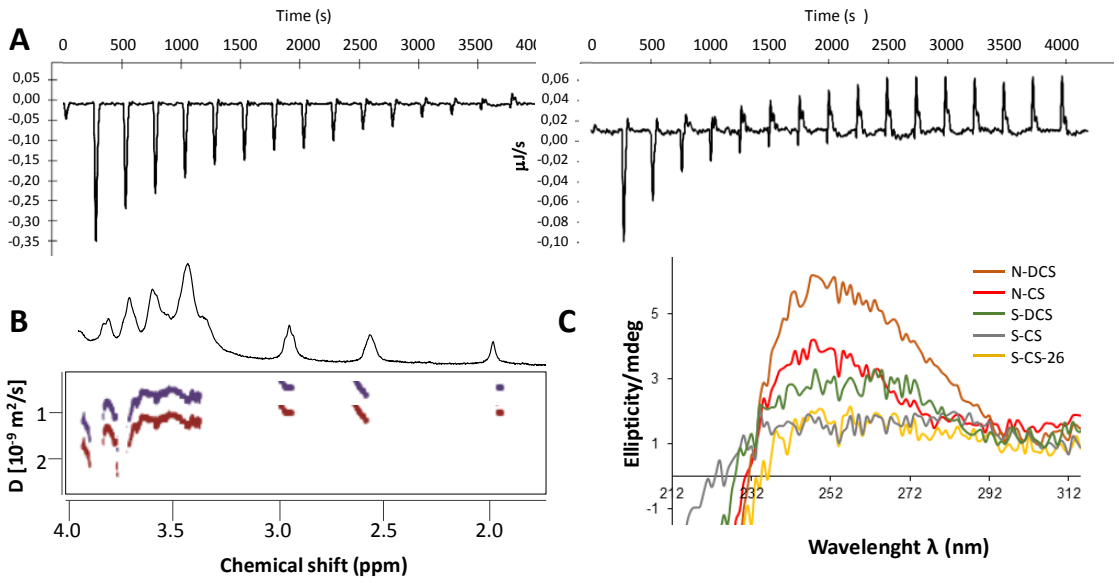

Figure 5. A. *ITC dilution experiments performed with* **S-CS** *(A) and* **N-CS** *(B).* ***B.*** *DOSY spectrum of* **N-CS** *at different concentrations (purple: 1 mg/mL and red: 0.01 mg/mL). The polysaccharide has a different translational diffusion coefficient when this was diluted at 25 ºC in D_2O, indicating the presence of soluble complexes at high concentrations.* ***C****. CD spectra of sulfated chitosan in PBS solution with a concentration of 20 mg/mL.* **N-DCS** *(red) exhibits clearly the highest ellipticity value, indicating a higher tertiary structure for this polymer.*

Diffusion ordered spectroscopy experiments (DOSY) indicate that translational diffusion coefficients of **N-CS** in D_2O at 25 ºC decrease when diluted conditions are employed (Figure 6).

Finally, to delve more deeply into these structural questions, circular dichroism (CD) studies were carried out (Figure 7). **S-CS** and **S-CS-26** did not have any visible bands. For N-sulfated chitosan (**N-CS** and **N-DCS**) and for **S-DCS** a positive band around 245 nm was observed. Interestingly, **N-DCS** exhibits the highest ellipticity value (+6 ellipticity/mdeg), indicating a higher tertiary structure for this polymer. Previous results[43] suggest that the polymer may adopt a helical (right-handed) secondary structure.

These diverse structures are in agreement with the non-correspondence between the zeta potential and the sulfation degree (Table 1).

3.3. Interaction of sulfated chitosan with growth factors.

Firstly, we analyzed the interaction capacity of the polysaccharides with different growth and neurotrophic factors (Figure 6A). Binding assays were performed in a standard fluorescence microplate reader using heparin (**Hp**) as control based on its availability and on its low price in comparison to heparan sulfates. The rapid ionic gelation of **N-CS** under the employed conditions prevented its use in these experiments.

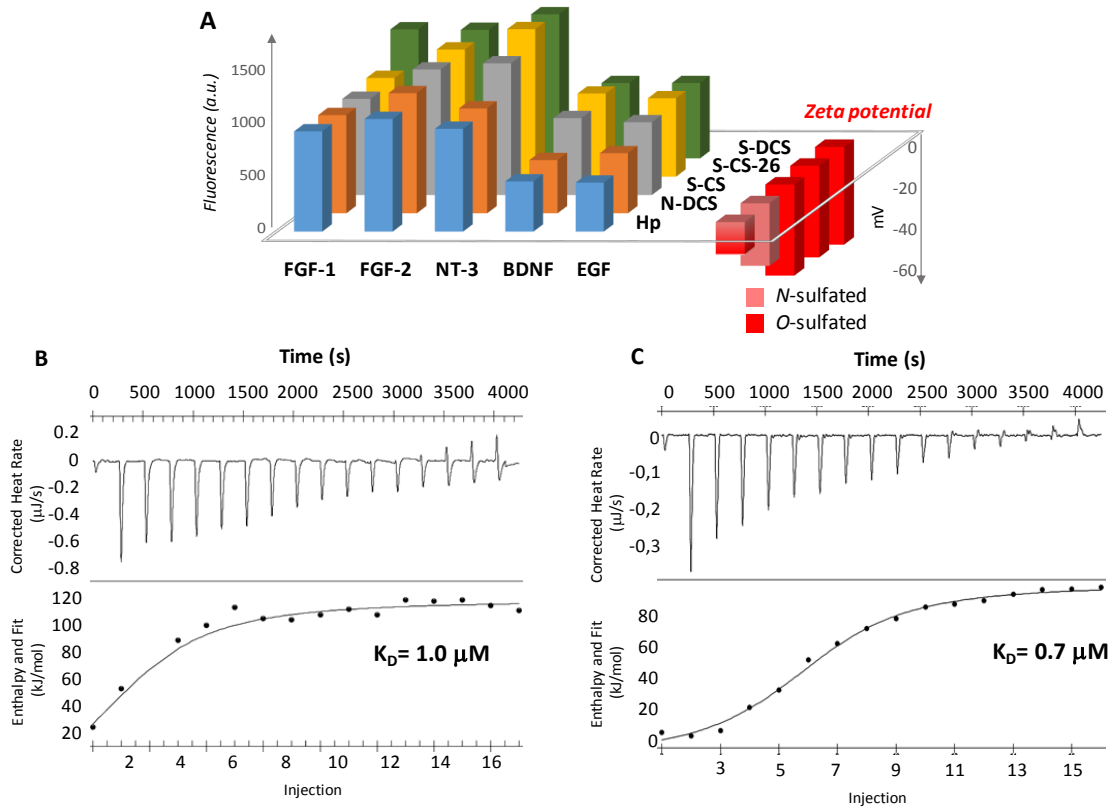

Figure 6. A. *Interaction of heparin (blue) chitosan sulfates (***N-DCS***: orange,* **S-CS***: grey,* **S-CS-26***: yellow,* **S-DCS***: green) with growth and neurotrophic factors (FGF-1, FGF-2, NT-3, BDNF, EGF). Zeta potential values are shown in the left.* ***B.*** *ITC titration experiments performed with* **N-DCS** *and* **S-DCS**. K_D *values are given in µM.*

The observed response was specific for each of the chitosan sulfate-GF pairs tested; nevertheless, some general conclusions could be deduced. Overall, **Hp** and synthetic

chitosan sulfates follow a similar pattern of interaction. Notably, they showed significantly greater interaction with FGF-1, FGF-2 and NT-3 than with BDNF and EGF.

On the other hand, *O*-sulfated CSs (**S-CS**, **S-DCS** and **S-CS-26**) belonged to the strongest binding partners for all growth factors and had a significantly higher affinity for them than the *N*-sulfated species (**Hp** and **N-DCS**) that were composed exclusively of N-sulfated or even *N*-sulfated/*O*-sulfated residues. These results suggest that the *O*-sulfated residues in the binding sequences can actively contribute to the intermolecular interaction of these with GFs.

However, if we assume that *O*-sulfate residues are predominant elements in the **Hp** composition, we can hypothesize that any marked alterations in the proportion of the *N*-sulfated and *O*-sulfated units can significantly modulate the binding potential through an influence on the conformational adaptation of the polysaccharide and/or the proper positioning of the sulfate residues.

According to the determined binding capacities, it is reasonable to postulate that O-sulfates are more adaptable than *N*-sulfates. However, a simple comparison between the "*degree of contraction*" values determined for **S-DCS** and **N-DCS** (Table 2) suggests that, despite a necessary conformation adaptation of the polysaccharide during the interaction process, the accessibility of sulfate groups for binding plays a crucial role in the interaction process.

In this context, a remarkable result was obtained for **Hp** and **N-DCS**. The binding capacity data were close, regardless of their substantially different degrees of sulfation. This similarity in the binding capacity of both polysaccharides could be explained by the fact that both have the lowest net charge on the surface as it is indicated by their zeta

potential values (fewer negatives). This is in accordance with our previously published results,[20,32] and highlights the key role of the net charge on the surface in the binding process.

To deepen our knowledge of these processes, we used ITC in two selected systems containing **S-DCS** and **N-DCS**. The data shown in Figure 6B did fit to a classical one-site binding model for the first injections. However, the observed switch from an exothermic to an endothermic process during the last injections at a well-defined composition ratio of sulfated chitosan did not fit to a classical model and can be interpreted as the result of the aggregation and subsequent coacervation of the complexes.[44] This characteristic multistage behavior has previously been observed when β-casein and mucin were titrated with chitosan.[34,44]

From these results, we envisaged that in the first injections the gradual addition of sulfated chitosan to the protein would result in the formation of complexes as an exothermic, enthalpy-driven process, resulting from heterotypic binding between the polymer and the growth factor. In both cases, this process was characterized by the same picks (13 injections) and the overall magnitude of the net integrated area of the exothermic component was similar for both sulfated chitosan (see Table S2). As the titration continued a saturation point was reached, beyond which heterotypic interactions with chitosan-growth factor no longer occurred when more ligand was added and endothermic peaks were observed. These inversion points suggest that the formation of chitosan sulfate/growth factor complexes occurs at a well-defined chitosan sulfate/growth factor proportion.

3.4. Influence of chitosan sulfates on *in vitro* cell proliferation/differentiation.

According to our results, chitosan sulfate variants with different structural motifs of the natural HSs are able to bind to the same GF. However, it is conceivable that the presence of these motifs can direct these polysaccharides to fulfill different biological functions by strictly determining their binding partner profile, as occurs in the natural GAGs. It is important to note that the action of HS mimics as GF ligands, appears to be context-dependent, adopting different mechanisms of action and, consequently, different biological effects depending on the cellular context.

With these considerations in mind, *in vitro* analysis was performed to determine the effects of different sulfated chitosan on the behavior of PC12 pheochromocytoma cells[45] and neural precursor cells from rat embryos cultures. In view of the possible future applications of these modified CSs, especially in the complex biological *in vivo* environment, we evaluated the cytotoxicity and the biodegradability of these unnatural polysaccharides (see Supporting Information, Figure S1 and S2). From our results, we can infer that polysaccharides have no toxicity to cells. Besides we have observed that sulfated chitosan are 1.5-2.0 times less biodegradable by lysozyme than that of **CS**, being their enzymatic hydrolysis rate controlled by the sulfation profile.

3.4.1. Effect of sulfated CSs on PC12 cells proliferation.

Recently, we[20] and others[22,46] have proposed that CSs as mimics of HPs can play a role in the proliferation/differentiation of cells, having hypothesized that the binding of GFs with their cell membrane receptors is enhanced by a low dose of CS, whilst an increase in concentration leads to inhibition of proliferation, presumably by sequestering the GF.

To gain insight into this dose-dependent effect we analyzed the effect of the polysaccharides in PC12 proliferation.

As can be observed in Figure 7, the dose-dependent effect cited previously occurs for **S-CS** and **S-DCS**. These slightly promote proliferation at the lowest concentrations (0.005-0.1 μg/mL), whilst the increase in concentration leads to proliferation inhibition. In contrast, re-acetylated polysaccharide **S-CS-26** exhibited anti-proliferative activity at all concentrations tested. Finally, the potency of **N-DCS** to enhance proliferation is much higher than **S-CS** and **S-DCS**. The break-over point (enhancing to inhibiting) occurred at the high concentration of 50 μg/mL. At concentrations below this, we observed a similar behavior to the **Hp**.

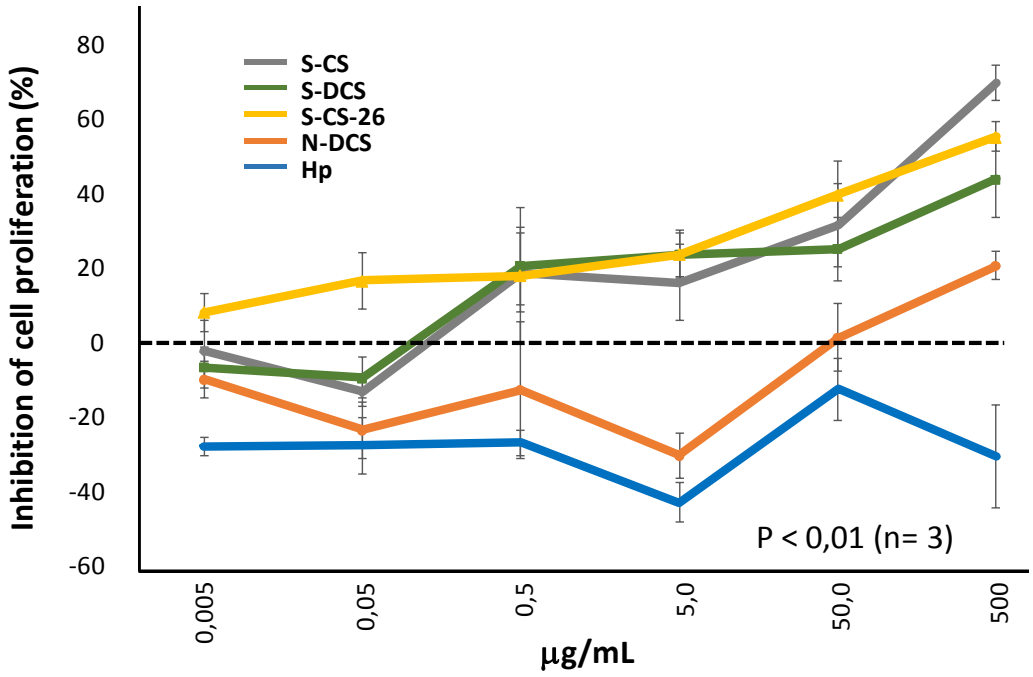

Figure 7. *Effect of sulfated CSs in PC-12 cell proliferation.* **Hp** *was used as control.*

These results suggest that *N*-sulfate motifs could be critical to activate the signaling pathways in PC12 cells proliferation, whilst *O*-sulfated CSs could preclude the interaction of the proteins with the corresponding cell membrane receptor, thus leading to the inhibition of cell proliferation. The effect of the polysaccharides correlates with

the zeta potential. In fact, compounds with the lowest zeta potential and lowest interaction capacity with FGF-2 (**Hp** and **N-DCS**) did not inhibit cell proliferation whilst a different effect has been observed with compounds that are highly charged on the surface (**S-CS**, **S-DCS** and **S-CS-26**).

Previous studies have proposed that although the electrical charge density determines the interaction between polyanionic polysaccharides and proteins, the unique properties of each protein-polysaccharide system are determined by other polysaccharide characteristics such as the chain flexibility.[31] The relatively high degree of contraction observed for **N-DCS** (32.0) reflects the flexible character of this macromolecule in comparison with **S-CS**, **S-DCS** and **S-CS-26** (9.6, 17.3, 13.8 respectively). These results and the known conformational flexibility of the **Hp** suggest that both macromolecules could allow the conformational molecular adaptation necessary for the specific formation of the ternary complex.

This interesting behavior could be related to the role of NS-domains on the cell surface or in the ECM.[8] Recent studies have demonstrated that flexible NS-domains are required for FGF-2 signaling,[47] suggesting a correlation between the *N*-sulfation degree and the FGF2·HS·FR1c complex formation.[48]

3.4.2. Effect of chitosan sulfates on neural precursor cells differentiation.

To study the effect of chitosan sulfates on cell differentiation we analyzed their effect in neural precursor cells (NPCs) cultures from rat embryos. Cells were cultured in a medium supplemented with 0.1 μg/mL of polysaccharide. Neural differentiation was studied by measuring the expression levels of GFAP(+)/Nestin(-), and βIII-

tubulin(+)/Nestin(-). Nestin is currently used as a marker of immature neural cells and GFAP(+) and βIII-tubulin(+) are astrocytic and neuron-specific markers, respectively.

As can be observed in Figure 8, the relative expression level of GFAP in chitosan sulfates-treated cells (0.1 μg/mL) was approximately five times greater than the level of βIII tubulin (Figures 8A and 8B). This suggests that more cells can be induced to astroglia than into neuron cells when they are treated with chitosan sulfates.

The *O*-sulfated **S-CS** and **S-CS-26** with higher M_w can better support the formation of astroglial cells. Evidenced for this can be seen in the greater expression of GFAP marker genes (Figure 8A) and the more altered cell morphology (Figures 8F and 8H), compared with the depolymerized **S-DCS** (Figure 8G). According to these results, the size of the polysaccharide chain exerts an influence on the promotion of cell differentiation of NPCs. A plausible explanation for this could be the fact that proliferation and neural differentiation are sequential and mutually exclusive processes as if crosstalk mechanisms exist that link the cell proliferation machinery and differentiation pathways. In this case, it can be supposed that if cells are treated with polymers with higher Mw (**S-CS** and **S-CS-26**) these could preclude more efficiently the interaction of the proteins with the corresponding cell membrane receptor thus leading to the inhibition of cell proliferation and allowing the cell to differentiate. However, the relative differentiation levels dropped when cells were treated with **S-DCS** which could indicate that a minimal chain size is necessary for achieving an efficient protein preclusion. In fact, previous studies have demonstrated the importance of **Hp** molecular weight to sequester GFs and their effect on stem cell differentiation.[49]

On the other hand, as shown in Figure 8A, cells treated with **N-DCS** (0.1 μg/mL) exhibited a relatively high differentiation level, despite its both relatively low molecular

weight and sulfation degree. In addition, the differentiation level showed an obvious dependence on the concentration (Figure 8J), exhibiting a maximum at this concentration whilst at higher concentrations the level declined.

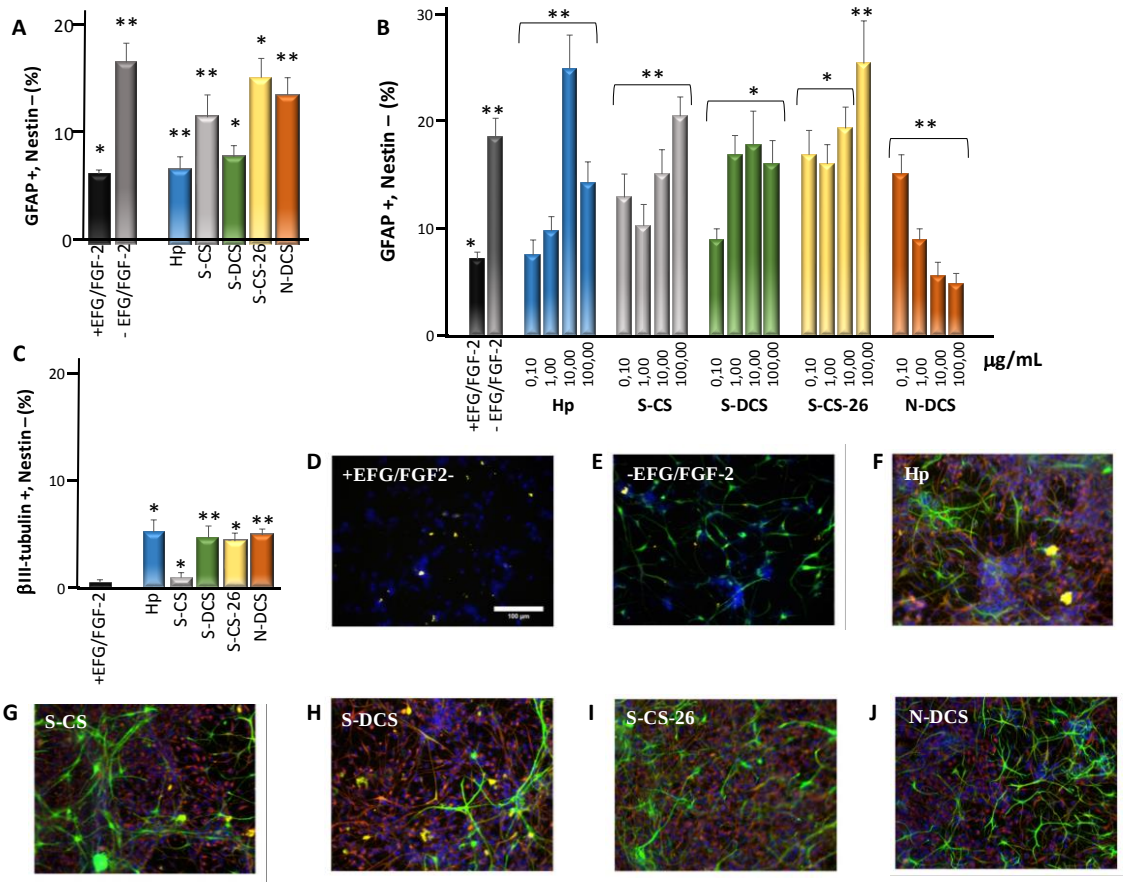

Figure 8. *Effect of sulfated chitosan and* **Hp** *(0.1 µg/mL) on neural differentiation of NPCs.* ***A****. Differential expression (%) in glia, using GFAP marker.* ***B****. Effect of concentration on glial cell differentiation of NPCs.* ***C****. Different expression (%) in neuron, using βIII-tubulin marker.* ***D-I****. Immunofluorescence images of NPCs correspond to GFAP, green; nestin, red and nuclei, blue. The EGF/FGF-2 were present in all treatments, cells treated only with these GFs or without them were used as control. Scale bar: 100 µm. * P < 0,001 (n= 3); ** P < 0,1 (n= 3).*

The idea that this polysaccharide could exhibit the best differentiation-promoting potential at this low concentration can be interpreted on the basis of the capacity of sulfated polysaccharides to form a ternary complex by directly interacting with both GF and its receptor and its dependence with the polysaccharide concentration. Recent studies have demonstrated the existence of an optimal concentration for the formation of

the ternary complex between the polysaccharide, the GF and its receptor.[17] As has been observed for **N-DCS** (Figure 8J), when concentrations are below this optimal concentration, the formation of the ternary complex can be effectively increased with increasing concentration, activating the signaling pathways in cells proliferation. These results demonstrated that there is an optimal concentration for inducing differentiation between 0.1 and 1.0 μg/mL for inducing differentiation, which is lower than the optimal concentration for **Hp** (5-10 μg/mL). Finally, it should be noted that although some polysaccharides at 0.1 μg/mL promoted βIII tubulin expression (Figure 8B), the expression at higher concentrations was minimal (see Supporting Information, Figure S3).

CONCLUSIONS

In this work, several heparanized chitosan with different properties (M_w, DA or DS) were prepared to mimic the sulfated domains of HS chains that are implicated in signaling events mediated by GFs. A combination of microviscosimetry, zeta potential analysis, isothermal titration calorimetry (ITC), diffusion ordered spectroscopy (DOSY), circular dichroism and fluorescence were employed to establish structure-function relationships. Our results highlight that the difference in the structure of heparan-mimicking chitosan would significantly influence their binding to GFs and are consistent with the hypothesis that interactions of sulfated chitosan with GFs are controlled by the combined effect of electrostatic interactions and the conformational adaptation of the polymer. Thus, we have found that highly charged O-sulfated **S-CS** and **S-DCS** polysaccharides with a low degree of contraction interacted more strongly with GFs that *N*-sulfated **N-DCS**, with a higher degree of contraction and a low charge.

Although the present study only represents an *in vitro* model and is an oversimplification of the phenomena occurring in vivo, these different degrees of interference of polysaccharides

with the GFs would significantly influence the promoting/inhibitory effects in cell proliferation/differentiation phenomena. Thus, the evidence gathered suggests that **N-DCS** would be able to bind to an allosteric zone and is likely to enhance GF signaling activity because the bound protein remains able to bind to its cognate receptor, promoting an effect on cell proliferation as has been shown for PC12 cells. However, **S-CS** and **S-DCS** would sequester the protein thus decreasing the GF signaling activity by depleting the protein or locally blocking its active site.

Therefore, our results contribute to recognizing the importance of the HS-domain topology in heparanized chitosan mimics and its decisive role on the orchestration of cellular responses.

ASSOCIATED CONTENT

Supporting Information. The following files are available free of charge.

A detailed description of the experimental methods together with the characterization of starting chitosan; cytotoxicity and biodegradability evaluation protocols and results and ITC results (.pdf).

AUTHOR INFORMATION

Corresponding author

Julia Revuelta - Departamento de Química Bio-Orgánica, Instituto de Química Orgánica General (IQOG-CSIC), CSIC, Juan de la Cierva 3, 28006 Madrid, Spain; ORCID: orcid.org/0000-0001-6225-7336; Email: julia.revuelta@iqog.csic.es

Authors

Inmaculada Aranaz - Departamento de Química en Ciencias Farmacéuticas, Facultad de Farmacia, Universidad Complutense de Madrid, Plaza de Ramón y Cajal, s/n, 28040 Madrid,

Spain. Instituto Pluridisciplinar. Universidad Complutense de Madrid, Paseo Juan XXIII, n128040 Madrid, Spain. ORCID: orcid.org/0000-0002-1495-9744.

Niuris Acosta - Departamento de Química en Ciencias Farmacéuticas, Facultad de Farmacia, Universidad Complutense de Madrid, Plaza de Ramón y Cajal, s/n, 28040 Madrid, Spain. Instituto Pluridisciplinar. Universidad Complutense de Madrid, Paseo Juan XXIII, n128040 Madrid, Spain. ORCID: orcid.org/0000-0003-4952-5935.

Concepción Civera - Departamento de Química en Ciencias Farmacéuticas, Facultad de Farmacia, Universidad Complutense de Madrid, Plaza de Ramón y Cajal, s/n, 28040 Madrid, Spain. ORCID: orcid.org/0000-0002-5684-7572.

Agatha Bastida - Departamento de Química Bio-Orgánica, Instituto de Química Orgánica General (IQOG-CSIC), CSIC, Juan de la Cierva 3, 28006 Madrid, Spain; ORCID: orcid.org/0000-0002-5141-9595.

Nerea Peña - Departamento de Química Bio-Orgánica, Instituto de Química Orgánica General (IQOG-CSIC), CSIC, Juan de la Cierva 3, 28006 Madrid, Spain.

Dianelis T. Monterrey - Departamento de Química Bio-Orgánica, Instituto de Química Orgánica General (IQOG-CSIC), CSIC, Juan de la Cierva 3, 28006 Madrid, Spain. ORCID: orcid.org/0000-0002-0227-8298.

Ernesto Doncel-Pérez - Laboratorio de Química Neuro-Regenerativa, Hospital Nacional de Parapléjicos, SESCAM, Finca la Peraleda s/n, 45071 Toledo, Spain. ORCID: orcid.org/0000-0002-2704-9782.

Leoncio Garrido - Departamento de Química-Física, Instituto de Ciencia y Tecnología de Polímeros, CSIC, Juan de la Cierva, 3, 28006, Madrid, Spain. ORCID: orcid.org/0000-0002-7587-1260.

Angeles Heras - Departamento de Química en Ciencias Farmacéuticas, Facultad de Farmacia, Universidad Complutense de Madrid, Plaza de Ramón y Cajal, s/n, 28040 Madrid,

Spain. Instituto Pluridisciplinar. Universidad Complutense de Madrid, Paseo Juan XXIII, n128040 Madrid, Spain. ORCID: orcid.org/0000-0002-7209-6190.

Eduardo García-Junceda - Departamento de Química Bio-Orgánica, Instituto de Química Orgánica General (IQOG-CSIC), CSIC, Juan de la Cierva 3, 28006 Madrid, Spain. ORCID: orcid.org/0000-0002-2344-8743.

Alfonso Fernández-Mayoralas - Departamento de Química Bio-Orgánica, Instituto de Química Orgánica General (IQOG-CSIC), CSIC, Juan de la Cierva 3, 28006 Madrid, Spain. ORCID: orcid.org/0000-0002-1241-7538.

Funding Sources

Grant MAT2015-65184-C2-1-R (MINECO/FEDER).

Grant MAT2015-65184-C2-2-R (MINECO/FEDER).

Grant PR87/19-22676 (Santander-UCM)

Notes

The authors declare no competing financial interest.

Acknowledgments

The authors gratefully acknowledge the financial support provided by the Spanish Ministerio de Economía y Competitividad (Grants MAT2015-65184-C2-1-R and MAT2015-65184-C2-2-R) and by Santander-UCM program (Grant PR87/19-22676). The authors acknowledge M.J. Macias and L. Ruiz (IRB Barcelona) for help and support with ITC experiments. N.P. acknowledge the Spanish National Research Council for a JAE-INTRO-ICUS fellowship.

References

1. Maddaluno, L.; Urwyler, C.; Werner, S. Fibroblast Growth Factors: Key Players in Regeneration and Tissue Repair. *Development* **2017**, *144*, 4047-4060.

2. Couchman, J. R.; Pataki, C. A. An Introduction to Proteoglycans and Their Localization. *J. Histochem. Cytochem.* **2012**, *60*, 885-897.

3. Rusnati, M.; Tanghetti, E.; Urbinati, C.; Tulipano, G.; Marchesini, S.; Ziche, M.; Presta, M. Interaction of Fibroblast Growth Factor-2 (FGF-2) with Free Gangliosides: Biochemical Characterization and Biological Consequences in Endothelial Cell Cultures. *Mol. Biol. Cell* **1999**, *10*, 313-327.

4. Ye, S.; Luo, Y.D.; Lu, W.Q.; Jones, R.B.; Linhardt, R.J.; Capila, I.; Toida, T.; Kan, M.; Pelletier, H.; McKeehan, W.L. Structural Basis for Interaction of FGF-1, FGF-2, and FGF-7 with Different Heparan Sulfate Motifs. *Biochemistry* **2001**, *40*, 14429-14439.

5. Bishop, J.R.; Schuksz, M.; Esko, J.D. Heparan Sulfate Proteoglycans Fine-Tune Mammalian Physiology. *Nature* **2007**, *446*, 1030-1037.

6. Gandhi, N.S.; Mancera, R.L. The Structure of Glycosaminoglycans and their Interactions with Proteins. *Chem. Biol. Drug Des.* **2008**, *72*, 455-482.

7. Gallagher, J. T. Multiprotein Signalling Complexes: Regional Assembly on Heparan Sulfate. *Biochem. Soc. Trans.* **2006**, *34*, 438-441.

8. Jastrebova, N.; Vanwildemeersch, M.; Lindahl, U.; Spillmann, D. Heparan Sulfate Domain Organization and Sulfation Modulate FGF-induced Cell Signaling. *J. Biol. Chem.* **2010**, *285*, 26842-26851.

9. Townley, R. A.; Bulow, H. E. Deciphering Functional Glycosaminoglycan Motifs in Development. *Curr. Opin. Struct. Biol.* **2018**, *50*, 144-154.

10. Koenig, A.; Norgard-Sumnicht, K.; Linhardt, R.; Varki, A. Differential Interactions of Heparin and Heparan Sulfate Glycosaminoglycans with the Selectins - Implications for the Use of Unfractionated and Low Molecular Weight Heparins as Therapeutic Agents. *J. Clin. Invest.* **1998**, *101*, 877-889.

11. Lambaerts, K.; Wilcox-Adelman, S. A.; Zimmermann, P. The Signaling Mechanisms of Syndecan Heparan Sulfate Proteoglycans. *Curr. Opin. Cell Biol.* **2009**, *21*, 662-669.

12. Seffouh, A.; El Masri, R.; Makshakova, O.; Gout, E.; Hassoun, Z.E.; Andrieu, J.P.; Lortat-Jacob, H.; Vives, R.R. Expression and Purification of Recombinant Extracellular Sulfatase HSulf-2 allows Deciphering of Enzyme Sub-domain Coordinated Role for the Binding and 6-O-Desulfation of Heparan Sulfate. *Cell. Mol. Life Sci.* **2019**, *76*, 1807-1819.

13. Mende, M.; Bednarek, C.; Wawryszyn, M.; Sauter, P.; Biskup, M.B.; Schepers, U.; Bräse, S. Chemical Synthesis of Glycosaminoglycans. *Chem. Rev.* **2016**, *116*, 8193-8255.

14. Bedini, E.; Laezza, A.; Parrilli, M.; Iadonisi, A. A Review of Chemical Methods for the Selective Sulfation and Desulfation of Polysaccharides. *Carbohydr. Polym.* **2017**, *174*, 1224-1239.

15. Li, J.; Cai, C.; Wang, L.H.; Yang, C.D.; Jiang, H.; Li, M.M.; Xu, D.; Li, G.Y.; Li, C.X.; Yu, G.L. Chemoenzymatic Synthesis of Heparan Sulfate Mimetic Glycopolymers and Their Interactions with the Receptor for Advanced Glycation End-Product. *ACS Macro Lett.* **2019**, *8*, 1570-1574.

16. Revuelta, J.; Fuentes, R.; Lagartera, L.; Hernáiz, M.J.; Bastida, A.; García-Junceda, E.; Fernández-Mayoralas, A. Assembly of Glycoamino Acid Building Blocks:

a New Strategy for the Straightforward Synthesis of Heparan Sulfate Mimics. *Chem. Comm.* **2018**, *54*, 13455-13458.

17. Lei, J.H.; Yuan, Y.Q.; Lyu, Z.L.; Wang, M.M.; Liu, Q.; Wang, H.W.; Yuan, L.; Chen, H. Deciphering the Role of Sulfonated Unit in Heparin-Mimicking Polymer to Promote Neural Differentiation of Embryonic Stem Cells. *ACS Appl. Mater. Inter.* **2017**, *9*, 28209-28221.

18. Zhang, G.L.; Ye, X.S. Synthetic Glycans and Glycomimetics: A Promising Alternative to Natural Polysaccharides. *Chem. Eur. J.* **2018**, *24*, 6696-6704.

19. Dimassi, S.; Tabary, N.; Chai, F.; Blanchemain, N.; Martel, B., Sulfonated and Sulfated Chitosan Derivatives for Biomedical Applications: A Review. *Carbohydr. Polym.* **2018,** *202*, 382-396.

20. Doncel-Pérez, E.; Aranaz, I.; Bastida, A.; Revuelta, J.; Camacho, C.; Acosta, N.; Garrido, L.; Civera, C.; García-Junceda, E.; Heras, A.; Fernández-Mayoralas, A. Synthesis, Physicochemical Characterization and Biological Evaluation of Chitosan Sulfate as Heparan Sulfate Mimics. *Carbohydr. Polym.* **2018,** *191*, 225-233.

21. Ding, K.; Wang, Y.; Wang, H.; Yuan, L.; Tan, M.; Shi, X.; Lyu, Z.; Liu, Y.; Chen, H. 6-*O*-Sulfated Chitosan Promoting the Neural Differentiation of Mouse Embryonic Stem Cells. *ACS Appl. Mater. Inter.* **2014**, *6*, 20043-20050.

22. Weltrowski, A.; da Silva Almeida, M.-L.; Peschel, D.; Zhang, K.; Fischer, S.; Groth, T. Mitogenic Activity of Sulfated Chitosan and Cellulose Derivatives is Related to Protection of FGF-2 from Proteolytic Cleavage. *Macromol. Biosci.* **2012**, *12*, 740-750.

23. Lavertu, M.; Xia, Z.; Serreqi, A.N.; Berrada, M.; Rodrigues, A.; Wang, D.; Buschmann, M. D.; Gupta, A. A Validated 1-H NMR Method for the Determination of the Degree of Deacetylation of Chitosan. *J. Pharm. Biomed. Anal.* **2003**, *32*, 1149-1158.

24. Holme, K.R.; Perlin, A. S. Chitosan *N*-sulfate. A Water-Soluble Polyelectrolyte. *Carbohydr. Res.* **1997**, *302*(1-2), 7-12.

25. Doncel-Pérez, E.; Caballero-Chacón, S.; Nieto-Sampedro, M. Neurosphere Cell Differentiation to Aldynoglia Promoted by Olfactory Ensheathing Cell Conditioned Medium. *Glia* **2009**, *57*, 1393-1409.

26. Hirata, Y. Manganese-Induced Apoptosis in PC12 Cells. *Neurotoxicol. Teratol.* **2002**, *24*, 639-653.

27. Virmani, A.; Gaetani, F.; Imam, S.; Binienda, Z.; Ali, S. Possible Mechanism for the Neuroprotective Effects of L-carnitine on Methamphetamine-Evoked Neurotoxicity. *Ann. N. Y. Acad. Sci.* **2003**, *993*, 197-207.

28. Wolf, C.; Bruss, M.; Hanisch, B.; Gothert, M.; von Kugelgen, I.; Molderings, G.J. Molecular Basis for the Antiproliferative Effect of Agmatine in Tumor Cells of Colonic, Hepatic, and Neuronal Origin. *Mol. Pharmacol.* **2007**, *71*, 276-283.

29. Yano, T.; Sugio, K.; Yamazaki, K.; Kase, S.; Yamaguchi, M.; Ondo, K.; Sugimachi, K. Direct IFNluence of Interferon-Gamma on Proliferation and Cell-Surface Antigen Expression of Non-Small Cell Lung Cancer Cells. *Lung cancer* **2000**, *30*, 169-174.

30. Griffin, C.C.; Linhardt, R.J.; Van Gorp, C.L.; Toida, T.; Hileman, R. E.; Schubert, R.L.; Brown, S. E. Isolation and Characterization of Heparan Sulfate from Crude Porcine Intestinal Mucosal Peptidoglycan Heparin. *Carbohydr. Res.* **1995**, *276* (1), 183-197.

31. Menchicchi, B.; Fuenzalida, J.P.; Hensel, A.; Swamy, M.J.; David, L.; Rochas, C.; Goycoolea, F.M. Biophysical Analysis of the Molecular Interactions between Polysaccharides and Mucin. *Biomacromolecules* **2015**, *16*, 924-935.

32. Benito-Arenas, R.; Doncel-Pérez, E.; Fernández-Gutiérrez, M.; Garrido, L.; García-Junceda, E.; Revuelta, J.; Bastida, A.; Fernández-Mayoralas, A. A Holistic Approach to Unravelling Chondroitin Sulfation: Correlations Between Surface Charge, Structure and Binding to Growth Factors. *Carbohydr. Polym.* **2018**, *202*, 211-218.

33. Pudelko, A.; Wisowski, G.; Olczyk, K.; Kozma, E.M. The Dual Role of the Glycosaminoglycan Chondroitin-6-Sulfate in the Development, Progression and Metastasis of Cancer. *FEBS J.* **2019**, *286*, 1815-1837.

34. Menchicchi, B.; Fuenzalida, J.P.; Bobbili, K.B.; Hensel, A.; Swamy, M.J.; Goycoolea, F.M. Structure of Chitosan Determines Its Interactions with Mucin. *Biomacromolecules* **2014**, *15*, 3550-3558.

35. McClements, D.J. Non-Covalent Interactions Between Proteins and Polysaccharides. *Biotechnol. Adv.* **2006**, *24*, 621-625.

36. Kudaibergenov, S.E.; Nuraje, N. Intra- and Interpolyelectrolyte Complexes of Polyampholytes. *Polymers* **2018**, *10*, 1146..

37. Terbojevich, M.; Carraro, C.; Cosani, A.; Focher, B.; Naggi, A. M.; Torri, G. Solution Studies of Chitosan 6-*O*-Sulfate. *Macromol. Chem. Phys.* **1989**, *190*, 2847-2855.

38. Cai, Z.; Chen, P.; Jin, H. J.; Kim, J. The Effect of Chitosan Content on the Crystallinity, Thermal Stability, and Mechanical Properties of Bacterial Cellulose-Chitosan Composites. *Proc. Inst. Mech. Eng., Part C* **2009,** *223*, 2225-2230.

39. Ogawa, K.; Yui, T.; Okuyama, K. Three D Structures of Chitosan. *Int. J. Biol. Macromol.* **2004**, *34*, 1-8.

40. Yang, Y.; Wang, S.; Wang, Y.; Wang, X.; Wang, Q.; Chen, M. Advances in Self-Assembled Chitosan Nanomaterials for Drug Delivery. *Biotechnol. Adv.* **2014**, *32*, 1301-1316.

41. Odunze, U.; O'Brien, F.; Godfrey, L.; Schatzlein, A.; Uchegbu, I. Unusual Enthalpy Driven Self Assembly at Room Temperature with Chitosan Amphiphiles. *Pharm. Nanotechnol.* **2019**, *7*, 57-71.

42. Kumar, S.; Koh, J. Physiochemical, Circular Dichroism-Induced Helical Conformation and Optical Property of Chitosan Azo-Based Amino Methanesulfonate Complex. *J. Appl. Polym. Sci.* **2012**, *124*, 4897-4903.

43. Turgeon, S. L.; Schmitt, C.; Sanchez, C. Protein–Polysaccharide Complexes and Coacervates. *Curr. Opin. Colloid In.* **2007**, *12*, 166-178.

44. Kasimova, M.R.; Velázquez-Campoy, A.; Nielsen, H.M. On the Temperature Dependence of Complex Formation between Chitosan and Proteins. *Biomacromolecules* **2011**, *12*, 2534-2543.

45. Attiah, D.G.; Kopher, R.A.; Desai, T.A., Characterization of PC12 Cell Proliferation and Differentiation-Stimulated by ECM Adhesion Proteins and Neurotrophic Factors. *J. Mater. Sci – Mater. M.* **2003**, *14*, 1005-1009.

46. Zeng, K.; Groth, T.; Zhang, K.. Recent Advances in Artificially Sulfated Polysaccharides for Applications in Cell Growth and Differentiation, Drug Delivery, and Tissue Engineering. *ChemBioChem* **2019**, *20*, 737 –746.

47. Schultz, V.; Suflita, M.; Liu, X. Y.; Zhang, X.; Yu, Y. L.; Li, L. Y.; Green, D. E.; Xu, Y. M.; Zhang, F. M.; DeAngelis, P. L.; Liu, J.; Linhardt, R. J., Heparan Sulfate Domains Required for Fibroblast Growth Factor 1 and 2 Signaling through Fibroblast Growth Factor Receptor 1c. *J. Biol. Chem.* **2017,** *292*, 2495-2509.

48. Jastrebova, N.; Vanwildemeersch, M.; Rapraeger, A.C.; Giménez-Gallego, G.; Lindahl, U.; Spillmann, D. Heparan Sulfate-related Oligosaccharides in Ternary Complex Formation with Fibroblast Growth Factors 1 and 2 and Their Receptors. *J. Biol. Chem.* **2006**, *281*, 26884-26892.

49. Jha, A. K.; Mathur, A.; Svedlund, F.L.; Ye, J.; Yeghiazarians, Y.; Healy, K.E. Molecular Weight and Concentration of Heparin in Hyaluronic Acid-based Matrices Modulates Growth Factor Retention Kinetics and Stem Cell Fate. *J. Control. Release* **2015**, *209*, 308-316.